Higher twist contributions to R-hadron phenomenology in the light gluino scenario

T.D. Gutierrez , R. Vogt , J.F. Gunion

Abstract

The open light gluino window allows non-trivial higher-twist gluino contributions to the proton wave function. Using a two-component model originally developed for charm hadroproduction, higher-twist intrinsic gluino contributions to final-state R-hadron formation are shown to enhance leading-twist production in the forward x_F region. We calculate R-hadron production at $p_{\rm lab}$ 800 GeV in pp, pBe, and pCu interactions with light gluino masses of 1.2, 1.5, 3.5, and 5.0 GeV.

PACS: 12.38.Bx; 13.75.Ev; 14.20.Lg; 14.40.Lb
Keywords: Charm meson and baryon hadroproduction

1. Introduction

The gluino is the supersymmetric partner of the gluon. It is an electromagnetically neutral, adjoint fermion with the same color structure as its boson counterpart. As yet, no clear experimental evidence of supersymmetric particles has been found. The most likely reason for this is the large expected mass of the supersymmetric particles ($\Lambda_{\rm SUSY} \sim 1$ TeV). However, an intriguing scenario exists whereby the gluino is not only the lightest supersymmetric particle but also very light compared to the SUSY scale, $m_{\tilde{g}} \ll 100$ GeV. This possibility arises naturally in a number of quite attractive models characterized by

special boundary conditions at the grand unification scale [1–3] and in certain models of gauge-mediated supersymmetry breaking [4,5].

Light gluinos are predicted to form relatively light bound states of quarks or gluons and gluinos called R-hadrons [6]. The lightest predicted R-hadrons include mesinos ($q\bar{q}\tilde{g}$), two barinos, $R^+(uud\tilde{g})$ and $S^0(uds\tilde{g})$ (and their anti-particles), gluinoballs ($\tilde{g}\tilde{g}$), and the glueballino, $R^0(\tilde{g}g)$. The properties of R-hadrons, including their mass, decay modes, and lifetimes, depend strongly on the mass of the gluino and on the mass of the lightest supersymmetric particle, which is typically the photino, $\tilde{\gamma}$, the supersymmetric partner of the photon. In the light gluino scenario, the mass of the R^0, the lightest R-hadron, is estimated to be $\approx 1-3$ GeV, or possibly somewhat larger. It is expected to decay dominantly to $\rho\tilde{\gamma}$, with $\rho \to \pi^+\pi^-$. Other possible decay channels for the R^0 include $\pi^+\pi^-\tilde{\gamma}$, $\eta\tilde{\gamma}$ and the C-violating mode $\pi^0\tilde{\gamma}$ [7–9]. The photino is predicted to be very weakly interacting and, in R-parity conserving supersymmetry, stable. As a result, the photino leads to "missing energy" in the detector. The other R-hadrons are expected to chain decay to the R^0. For instance, the R^+ is expected to decay to $S^0\pi^+$. The S^0 then decays to $R^0\Lambda$, if kinematically allowed given the 1.41 GeV mass of the Λ [1,2], or, alternatively, directly to $\rho\Lambda\tilde{\gamma} + \cdots$. The R^+ is expected to be somewhat more massive than the R^0 with a mass of $\approx 1.6-3.1$ GeV while the S^0 is predicted to be about 200 MeV lighter than the R^+. Thus, the key to ruling out or finding evidence for the light gluino scenario is the ability to detect the R^0 (through its $\rho\tilde{\gamma}$ decay mode) possibly in association with a pion and/or a Λ. This is challenging, especially because of the invisibility of the $\tilde{\gamma}$ which prevents reconstruction of a mass peak.

There have been many theoretical and experimental attempts to find evidence for and/or exclude the light gluino scenario. Searches for R-hadrons produced in fixed target experiments have been performed for a number of the predicted R-hadron decay channels [7–10]. Effects of a light gluino on QCD observables have been analyzed [11–15]. Stable particle searches, Υ decays, beam dump experiments etc. all have potential sensitivity to the presence of a light gluino or the R-hadrons. A brief summary of the various possible resulting constraints on a light gluino is given in Ref. [16]. In addition, Ref. [17] claims that $m_{\tilde{g}} > 2.5-3$ GeV is excluded on the basis of their analysis of OPAL data. Although these various analyses are, in combination, potentially sensitive to most regions of light gluino mass, all rely on model-dependent inputs. As a result, we believe that at present it is impossible to *definitively* exclude any gluino mass below $4-5$ GeV. Thus, it is of great interest to find additional approaches for discovering and/or constraining light gluinos and the R-hadrons.

In this paper, we will explore the possibility of detecting R-hadrons at large x_F in pp and pA fixed-target interactions. Our calculations will be restricted to the $m_{\tilde{g}} \sim 1.2-5$ GeV region where we can be confident that the semi-perturbative techniques that we employ are reliable. This region is of particular phenomenological interest because of the analogy that can be drawn between heavy quark and light gluino production. Indeed, if the gluino and heavy quark masses are comparable, one might anticipate observation of hard gluino production analogous to that already observed in high x_F charm hadroproduction [18–24]. The leading-twist pQCD predictions for charm production in pp and pA collisions

fail to account for many features of the high x_F data. These include unexpectedly large production rates and anomalies such as flavor correlations between the produced hadrons and the valence spectators, manifested as leading charm and a strong D^+/D^- asymmetry in $\pi^- A$ interactions [18–24], double J/Ψ production at large x_F [25,26], and Feynman scaling of J/Ψ production in pA interactions [27–29], all of which suggest a breakdown of factorization [30–33] at large x_F. The anomalies and cross section enhancement may be partly explained by higher-twist terms in the operator product expansion (OPE) on the light cone associated with the dynamics of the QCD bound state. Analogous terms should be present for light gluinos.

The intrinsic charm model (IC) [34–36] approximates non-perturbative higher-twist Fock state contributions of heavy quarks in hadronic wave functions. The phenomenological predictions of IC directly address the above puzzles in charm hadroproduction [37–42]. For example, IC provides a coalescence mechanism whereby final-state hadrons can share valence quarks with the projectile, naturally producing leading particles.

In analogy with leading charm, we study R-hadron distributions using "intrinsic gluinos" ($I\widetilde{G}$) in regions of phase space where the gluino mass and momentum fractions conspire so that higher-twist effects cannot be ignored. In this paper, we calculate enhancements over the leading-twist R-hadrons x_F distributions with gluino masses $m_{\tilde{g}} =$ 1.2, 1.5, 3.5, and 5.0 GeV. Both pp and pA interactions at $p_{\rm lab} = 800$ GeV are considered. For many cases, the enhancements of R-hadron production at large x_F are sufficiently substantial that a significant excess above normal expectations of high x_F ρ, π, and Λ production might very well be observed if the gluino is light.

2. pQCD light gluino hadroproduction

In pQCD, gluinos are produced in pairs by gg fusion and $q\bar{q}$ annihilation, $gg, q\bar{q} \to \tilde{g}\tilde{g}$, as well as quark–gluon scattering to squark and gluino, $qg \to \tilde{q}\tilde{g}$. Precision Z-pole data has constrained the squark mass to be greater than 100 GeV, quite large compared to the light gluino masses considered here. Therefore, we expect that the qg contribution with the virtual squark in the t-channel will be small compared to the other contributions, particularly at fixed-target energies.

The leading-twist inclusive R-hadron x_F distribution at leading order is obtained from the gluino x_F distribution ($x_F = (2m_T/\sqrt{s})\sinh y$) which has the factorized form in pQCD

$$\frac{d\sigma}{dx_F} = \sum_{i,j} \frac{\sqrt{s}}{2} \int dz_3\, dy_2\, d^2p_T\, \frac{1}{E_1} \frac{D_{H/\tilde{g}}(z_3)}{z_3} f_i^A(x_a) f_j^B(x_b) \frac{1}{\pi} \frac{d\hat{\sigma}_{ij}}{d\hat{t}}. \tag{1}$$

Here a and b are the initial partons from projectile and target hadrons A and B, 1 and 2 are the produced gluinos, and 3 is the final-state R-hadron. The sum over i and j extends over all partonic gluino production subprocesses. A K factor of 2.5 is included to account for NLO corrections. Since the K factor is approximately constant with x_F for charm production except as $x_F \to 1$, we assume that the K factor for gluino production is also independent of x_F.

The fragmentation functions, $D_{H/\tilde{g}}(z)$ with $z = x_H/x_{\tilde{g}}$, describe the collinear fragmentation of final-state R-hadrons from the produced gluinos. For simplicity, a delta function was used for hadronization, $D_{H/\tilde{g}}(z) = \delta(z-1)$. This assumption results in the hardest x_F distribution at leading-twist since the R-hadron carries all of the gluino's momentum. Other fragmentation functions would soften these distributions. Note that for any fragmentation function to factorize, it must be independent of the initial state (i.e., it only depends on z_3 and not x_a). Thus, regardless of the fragmentation function used, all R-hadrons will be decoupled from the initial state to leading-twist.

The partonic cross sections for gluino production in Eq. (1) are [43]

$$\begin{aligned}\frac{d\hat{\sigma}_{gg\to\tilde{g}\tilde{g}}}{d\hat{t}} = \frac{9\pi\alpha_s^2}{4\hat{s}^2}\Bigg[&\frac{2(m_{\tilde{g}}^2-\hat{t})(\hat{u}-m_{\tilde{g}}^2)}{\hat{s}^2} + \frac{m_{\tilde{g}}^2(\hat{s}-4m_{\tilde{g}}^2)}{(m_{\tilde{g}}^2-\hat{t})(\hat{u}-m_{\tilde{g}}^2)} \\ &+ \frac{(m_{\tilde{g}}^2-\hat{t})(\hat{u}-m_{\tilde{g}}^2) - 2m_{\tilde{g}}^2(m_{\tilde{g}}^2+\hat{t})}{(m_{\tilde{g}}^2-\hat{t})^2} \\ &+ \frac{(m_{\tilde{g}}^2-\hat{t})(\hat{u}-m_{\tilde{g}}^2) + m_{\tilde{g}}^2(\hat{u}-\hat{t})}{\hat{s}(m_{\tilde{g}}^2-\hat{t})} \\ &+ \frac{(m_{\tilde{g}}^2-\hat{u})(\hat{t}-m_{\tilde{g}}^2) - 2m_{\tilde{g}}^2(m_{\tilde{g}}^2+\hat{u})}{(m_{\tilde{g}}^2-\hat{u})^2} \\ &+ \frac{(m_{\tilde{g}}^2-\hat{u})(\hat{t}-m_{\tilde{g}}^2) + m_{\tilde{g}}^2(\hat{t}-\hat{u})}{\hat{s}(m_{\tilde{g}}^2-\hat{u})}\Bigg], \end{aligned} \tag{2}$$

$$\begin{aligned}\frac{d\hat{\sigma}_{q\bar{q}\to\tilde{g}\tilde{g}}}{d\hat{t}} = \frac{\pi\alpha_s^2}{\hat{s}^2}\Bigg[&\frac{8}{3}\frac{(m_{\tilde{g}}^2-\hat{t})^2 + (\hat{u}-m_{\tilde{g}}^2)^2 + 2m_{\tilde{g}}^2\hat{s}}{\hat{s}^2} \\ &+ \frac{32}{27}\frac{(m_{\tilde{g}}^2-\hat{t})^2}{(m_{\tilde{q}}^2-\hat{t})^2} + \frac{32}{27}\frac{(\hat{u}-m_{\tilde{g}}^2)^2}{(\hat{u}-m_{\tilde{q}}^2)^2} + \frac{8}{3}\frac{(m_{\tilde{g}}^2-\hat{t})^2 + m_{\tilde{g}}^2\hat{s}}{\hat{s}(\hat{t}-m_{\tilde{q}}^2)} \\ &+ \frac{8}{27}\frac{m_{\tilde{g}}^2\hat{s}}{(m_{\tilde{q}}^2-\hat{t})(\hat{u}-m_{\tilde{q}}^2)} + \frac{8}{3}\frac{(\hat{u}-m_{\tilde{g}}^2)^2 + m_{\tilde{g}}^2\hat{s}}{\hat{s}(\hat{u}-m_{\tilde{q}}^2)}\Bigg], \end{aligned} \tag{3}$$

$$\begin{aligned}\frac{d\hat{\sigma}_{gq\to\tilde{q}\tilde{g}}}{d\hat{t}} = \frac{\pi\alpha_s^2}{\hat{s}^2}\Bigg[&\frac{4}{9}\frac{m_{\tilde{g}}^2-\hat{t}}{\hat{s}} + \frac{(m_{\tilde{g}}^2-\hat{t})\hat{s} + 2m_{\tilde{g}}^2(m_{\tilde{q}}^2-\hat{t})}{(m_{\tilde{g}}^2-\hat{t})^2} \\ &+ \frac{4}{9}\frac{(\hat{u}-m_{\tilde{g}}^2)(\hat{u}+m_{\tilde{q}}^2)}{(\hat{u}-m_{\tilde{q}}^2)^2} - \frac{(\hat{s}-m_{\tilde{q}}^2+m_{\tilde{g}}^2)(m_{\tilde{q}}^2-\hat{t}) - m_{\tilde{g}}^2\hat{s}}{\hat{s}(m_{\tilde{g}}^2-\hat{t})} \\ &+ \frac{1}{18}\frac{\hat{s}(\hat{u}+m_{\tilde{g}}^2) + 2(m_{\tilde{q}}^2-m_{\tilde{g}}^2)(m_{\tilde{g}}^2-\hat{u})}{\hat{s}(\hat{u}-m_{\tilde{q}}^2)} + \frac{1}{2}\frac{(m_{\tilde{q}}^2-\hat{t})(2\hat{u}+m_{\tilde{g}}^2+\hat{t})}{2(\hat{t}-m_{\tilde{g}}^2)(\hat{u}-m_{\tilde{q}}^2)} \\ &+ \frac{1}{2}\frac{(m_{\tilde{g}}^2-\hat{t})(\hat{s}+2\hat{t}-2m_{\tilde{q}}^2)}{2(\hat{t}-m_{\tilde{g}}^2)(\hat{u}-m_{\tilde{q}}^2)} + \frac{1}{2}\frac{(\hat{u}-m_{\tilde{g}}^2)(\hat{t}+m_{\tilde{g}}^2+2m_{\tilde{q}}^2)}{2(\hat{t}-m_{\tilde{g}}^2)(\hat{u}-m_{\tilde{q}}^2)}\Bigg]. \end{aligned} \tag{4}$$

We calculate leading-twist pQCD gluino distributions for 800 GeV pp interactions.

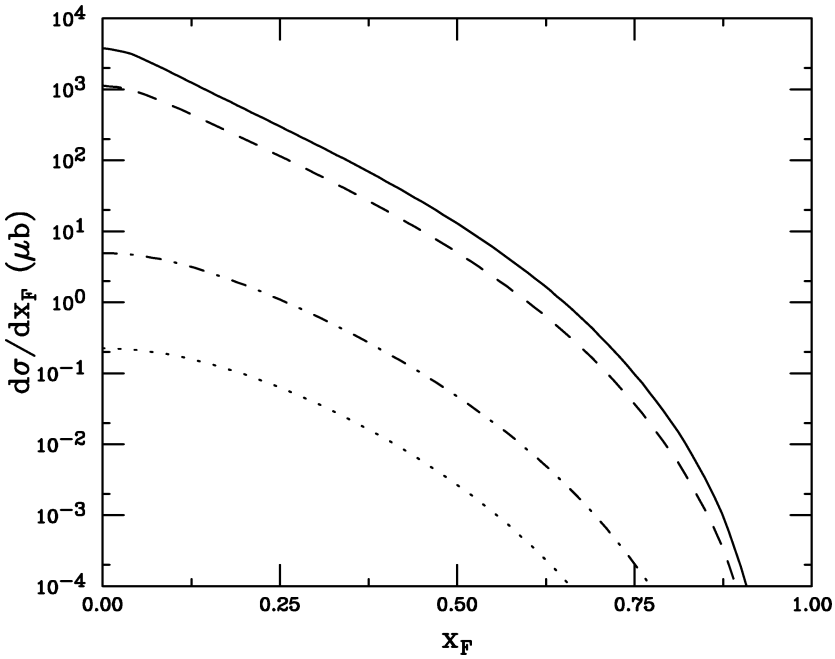

Fig. 1. 800 GeV QCD pp gluino production for several gluino masses. The curves are $m_{\tilde{g}} = 1.2$ GeV (solid), 1.5 GeV (dashed), 3.5 GeV (dot-dashed), and 5.0 GeV (dotted).

Fig. 1 shows the gluino distributions using the MRS D-parton distributions in the proton [44] with $m_{\tilde{g}} = 1.2, 1.5, 3.5$, and 5.0 GeV and $m_{\tilde{q}} = 100$ GeV. The characteristic falloff at large x_F is similar to heavy quark production. Choosing a larger squark mass would only marginally decrease the total cross section because the gq channel is suppressed by the large squark mass. The gluino production cross section is a strong function of mass. The cross section is largest for $m_{\tilde{g}} = 1.2$ GeV and decreases by a factor of 3 for $m_{\tilde{g}} = 1.5$ GeV. There is then a drop of 250 to the $m_{\tilde{g}} = 3.5$ GeV gluino cross section and another factor of 20 between the 3.5 and 5 GeV cross sections. Additionally, the falloff of the cross section with x_F becomes steeper as $m_{\tilde{g}}$ is increased.

Charm hadroproduction phenomenology has taught us that higher-twist contributions can become comparable to leading twist in certain parts of phase space, introducing correlations between the initial and final states. These effects will be addressed in the next section.

3. Intrinsic contribution to higher twist

In deep inelastic scattering, higher-twist terms in the OPE are suppressed by a factor of $1/Q^{2n}$. These terms are essentially irrelevant when Q^2 is large. Analogously, in hadroproduction, a similar suppression of $1/M^2$ typically renders higher-twist effects unimportant except in regions where pQCD is seemingly inapplicable (i.e., where M^2

is small). However, it has been shown that in the simultaneous $M^2 \to \infty$ and $x \to 1$ limit with $M^2(1-x)$ fixed, a new hard scale emerges where higher-twist contributions to the cross section become comparable to leading twist [45–47]. In the case of heavy quark production, this new scale can be associated with either the resolution of the transverse size of the intrinsic heavy quark pair or with the transverse resolution of any "pre-coalesced" hadrons inside the parent hadron. The heavy quark fluctuations can carry a large fraction of the projectile's forward momentum since the constituents of the bound state move with the same velocity. The Fock state may be broken up by an interaction with soft gluons in the target, producing a leading hadron containing a heavy parton.

The bound state wave function for a state containing higher-twist contributions can be obtained from the Bethe–Saltpeter formalism evaluated at equal "time" on the light cone [34,35,48]:

$$\left(M^2 - \sum_{i=1}^{n} \frac{\widehat{m}_i^2}{x_i}\right)\Psi(x_i, k_{T_i}) = \int_0^1 [dy] \int \frac{[d^2 l_T]}{16\pi^2} \widetilde{K}\big(x_i, k_{T_i}; y_i, l_{T_i}; M^2\big)\Psi(y_i, l_{T_i}), \tag{5}$$

where M is the mass of the projectile hadron. The transverse mass of an individual parton is defined by $\widehat{m}_i^2 = k_{T_i}^2 + m_i^2$, where k_{T_i} is the transverse momentum of the ith parton in the n-particle Fock state, $|q_1, \ldots, q_i, \ldots, q_n\rangle$. The momentum fraction of the ith parton in the Fock state is x_i, $[dy] = \prod_{i=1}^{n} dy_i\, \delta(1 - \sum_{i=1}^{n} y_i)$ is a longitudinal momentum conserving metric and $[d^2 l_T] = \prod_{i=1}^{n} d^2 l_{T_i}\, \delta^2(\sum_{i=1}^{n} \vec{l}_{T_i})$. The interaction kernel is $\widetilde{K}$.

The simplest way to create final-state hadron distributions from a specific Fock state wave function is now described. The vertex function on the right-hand side of Eq. (5) is assumed to be slowly varying with momentum. The operator on the left-hand side of the equation is then evaluated at the average transverse momentum of each parton, $\langle k_{T_i}^2 \rangle$, with the constraint $\sum_i^n \vec{k}_{T_i} = 0$. With these assumptions, the transverse mass of each parton is fixed and the vertex function becomes constant. The probability distribution is then proportional to the square of the wave function which is now inversely proportional to the off-shell parameter $\Delta = M^2 - \sum_{i=1}^{n} \langle \widehat{m}_i^2 \rangle / x_i$ where $\langle \widehat{m}_i^2 \rangle$ is the average transverse mass squared of the ith parton. After longitudinal momentum conservation is specified by $\delta(1 - \sum_{i=1}^{n} x_i)$, the probability distribution becomes

$$\frac{d^n P_n(x_1, \ldots, x_n)}{\prod_{i=1}^{n} dx_n} = N_n \delta\left(1 - \sum_{i=1}^{n} x_i\right) \Delta^{-2}, \tag{6}$$

where N_n is the normalization constant for an n-particle distribution. The probability distributions as a function of x for any final-state hadron can be generated by integrating Eq. (6) including final-state coalescence constraints.

The characteristic shape of the longitudinal momentum distribution of the final-state hadron can now be obtained up to an overall normalization constant. The important feature of this model is that final-state particles are not "produced" in a collision, as such, but are rather "intrinsic" to the projectile's Fock state and are liberated after a soft interaction with

the target. This intrinsic source of final-state particles acts as a perturbation to the dominant parton fusion mechanism. However, unlike parton fusion, it incorporates flavor correlations between the initial and final states. This mechanism will dominate the total cross section in the limit $x_F \to 1$ since $x_F \sim x$ when the final-state hadron evolves directly from the projectile wave function.

In this paper, we assume that the model developed for heavy quark hadroproduction at higher-twist can be applied to gluino production in the proton wave function. Final-state R-hadron production from $\widetilde{\mathrm{IG}}$ states is described in the remainder of this section along with its relationship to IC production. The characteristic shapes of the intrinsic distributions in the proton were generated for the gluino alone and for the $R^+(uud\tilde{g})$ and $S^0(uds\tilde{g})$, and the $R^0(g\tilde{g})$. In all cases, the "minimal Fock state" was used to generate the final state coalescence. This emphasizes the most leading final-states.

The gluino can fragment into a R-hadron, just as in pQCD production. In this uncorrelated case [49], the hadron x_F distribution is

$$\frac{dP_{i\tilde{g}}^{kF}}{dx_H} = N_k \int \prod_{j=1}^{k} dx_j\, dz\, \delta\left(1 - \sum_{i=1}^{k} x_i\right) \frac{D_{H/\tilde{g}}(z)}{z} \delta(x_H - z x_{\tilde{g}}) \Delta^{-2}, \tag{7}$$

where k indicates the order of the Fock state containing the intrinsic gluinos (i.e., the $x_{\tilde{g}}$'s are included among the x_i). Gluinos are produced in pairs because other supersymmetric vertices involving squarks and photinos are highly suppressed due to their much greater masses. The minimal proton Fock state with a gluino pair then has five particles, $|uud\tilde{g}\tilde{g}\rangle$. Fragmentation of other, higher, Fock states will have a smaller production probability and produce gluinos with lower average momentum. For consistency with the coalescence production described below, we include fragmentation of six- and seven-particle Fock states with R^0 and S^0 production, respectively.

R-hadron production by coalescence is specific to each hadron. The intrinsic gluino Fock states are fragile and can easily collapse into a new hadronic state through a soft interaction with the target, as is the case for IC states. The coalescence function is assumed to be a delta function. The momentum fraction of the final-state hadron is the sum of the momentum fractions of the R-hadron valence constituents from the proton wave function. The three R-hadrons we consider are all calculated from only the minimal Fock state required for their production by coalescence. Thus, only the most leading configuration is used. As in the fragmentation case in Eq. (7), including higher Fock components does not significantly increase the total rate because the other Fock state probabilities are smaller and also does not enhance the yield at large x_F because the average x_F of coalescence is reduced relative to that from the minimal Fock state.

The five-particle Fock state $|uud\tilde{g}\tilde{g}\rangle$ produces the most leading R-hadron, the R^+, because the R^+ is generated from four of the five constituents of the Fock state.

$$\frac{dP_{i\tilde{g}}^{5C}}{dx_{R^+}} = N_5 P_C^5 \int \prod_{j=1}^{5} dx_j\, \delta\left(1 - \sum_{i=1}^{5} x_i\right) \delta(x_{R^+} - x_u - x_u - x_d - x_{\tilde{g}}) \Delta^{-2}. \tag{8}$$

Here, P_C^5 is a factor incorporating the coalescence probability given the five-constituent Fock state. Note that in this case, the R^+ x_F distribution is proportional to the gluino distribution in Eq. (7), obtained by setting $D_{H/\tilde{g}}(z) = \delta(1-z)$, with $k=5$ evaluated at $1-x_F$.

The R^0 is generated from a six-particle Fock state, $|uudg\tilde{g}\tilde{g}\rangle$. Unlike the gluinos, single gluons can be included in the higher-twist Fock state since one gluon can couple to two quarks in the Fock state. The six-particle state is the most leading state for R^0 production. The coalescence of R^0 hadrons is described by

$$\frac{dP_{i\tilde{g}}^{6C}}{dx_{R^0}} = N_6 P_C^6 \int \prod_{j=1}^{6} dx_j \, \delta\Big(1 - \sum_{i=1}^{6} x_i\Big) \delta(x_{R_0} - x_g - x_{\tilde{g}}) \Delta^{-2}. \tag{9}$$

The last R-hadron we consider is the S^0 which, since it contains an s quark, must be produced from a seven-particle Fock state, $|uuds\bar{s}\tilde{g}\tilde{g}\rangle$. The S^0 will have a harder x_F distribution than the R^0 even though the average momentum fraction of each constituent in the seven-particle state is smaller than those of the six-particle state. This harder x_F distribution is due to the greater number of S^0 constituents, four, rather than the two R^0 constituents. In this case,

$$\frac{dP_{i\tilde{g}}^{7C}}{dx_{S^0}} = N_7 P_C^7 \int \prod_{j=1}^{7} dx_j \, \delta\Big(1 - \sum_{i=1}^{7} x_i\Big) \delta(x_{S_0} - x_u - x_d - x_s - x_{\tilde{g}}) \Delta^{-2}. \tag{10}$$

In what follows, the coalescence probabilities $P_C^{5,6,7}$ appearing in Eqs. (8)–(10) are taken to be unity. That is, it is assumed that the gluinos will always coalesce.

Fig. 2 shows (using arbitrary normalization) the characteristic x dependence of the probability distributions in Eqs. (7)–(10) with $m_{\tilde{g}} = 1.2$ GeV. The single gluino distribution is calculated using $k=5$ and $D_{H/\tilde{g}}(z) = \delta(1-z)$ in Eq. (7). R-hadrons produced by uncorrelated fragmentation have the softest x_F distributions, $\langle x_{\tilde{g}} \rangle = 0.24$ when $k=5$. Contributions from progressively higher single gluino Fock states have smaller relative probabilities, as we discuss below, and a decreased $\langle x_{\tilde{g}} \rangle$, which would eventually build up a gluino sea in the proton. The distributions from coalescence are all forward of the single gluino distribution. As expected, since the R^+ takes all three of the proton valence quarks, it is the most leading R-hadron with $\langle x_{R^+} \rangle = 0.76$. The distributions for the other final-state particles, the S_0 and the R_0, are softer with $\langle x_{S^0} \rangle = 0.56$ and $\langle x_{R^0} \rangle = 0.35$, respectively.

We have shown the results with the lowest gluino mass we consider. Increasing the mass increases the average x_F of the gluino distribution of uncorrelated fragmentation, Eq. (7), but leaves the average x_F of the R-hadrons unchanged in the mass range we consider.

The intrinsic gluino production cross section for R-hadrons, from an n-particle Fock state is written by analogy with the IC cross section

$$\sigma_{i\tilde{g}}^n(pp) = G_C P_{i\tilde{g}}^n \alpha_s^4(m_{\tilde{g}\tilde{g}}) \sigma_{pp}^{\text{in}} \frac{\mu^2}{4\widehat{m}_{\tilde{g}}^2}, \tag{11}$$

where G_C is a color factor. The inelastic pp cross section is ~ 35 mb at 800 GeV. The ratio $\mu^2/4\widehat{m}_{\tilde{g}}^2$ sets the scale at which the higher- and leading-twist contributions are comparable.

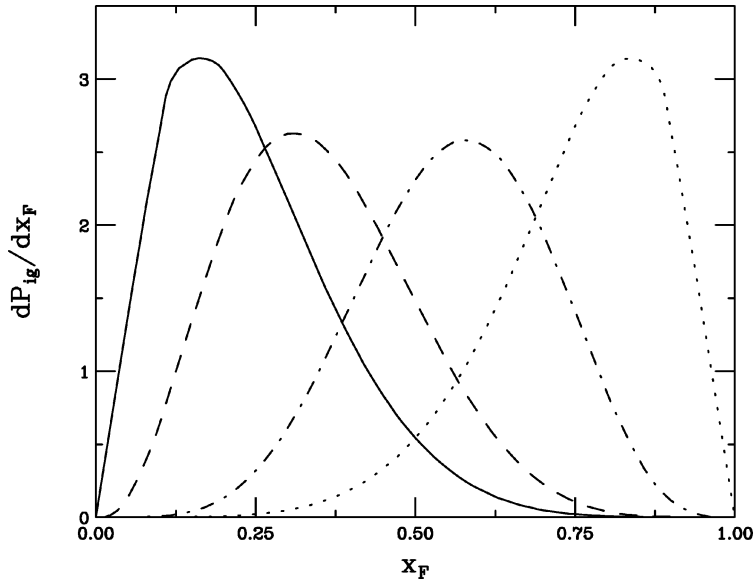

Fig. 2. The x distribution of intrinsic R-hadrons in the proton with $m_{\tilde{g}} = 1.2$ GeV. The curves are $\tilde{g}$ (solid), R^0 (dashed), S^0 (dot-dashed), and R^+ (dotted).

We use $\mu^2 \sim 0.2$ GeV^2, consistent with attributing the diffractive fraction of the total J/ψ production cross section to IC [37,38,42]. There is a factor of α_s^4 because the intrinsic state couples to two of the projectile valence quarks. The higher-twist contribution then contains two more powers of α_s than the leading-twist contribution. This factor is included in the cross section rather than in the probability distributions as done previously [38,42] to more explicitly show the effect of this dependence on the cross section when the mass of the intrinsic state is changed.

Since the intrinsic charm cross section is [38]

$$\sigma_{ic}^n(pp) = P_{ic}^n \alpha_s^4(m_{c\bar{c}}) \sigma_{pp}^{\rm in} \frac{\mu^2}{4\widehat{m}_c^2} \ , \tag{12}$$

the two cross sections are related by

$$\frac{\sigma_{i\tilde{g}}^n(pp)}{\sigma_{ic}^n(pp)} = \frac{G_C P_{i\tilde{g}}^n}{P_{ic}^n} \frac{\widehat{m}_c^2}{\widehat{m}_{\tilde{g}}^2} \frac{\alpha_s^4(m_{\tilde{g}\tilde{g}})}{\alpha_s^4(m_{c\bar{c}})}. \tag{13}$$

The relative color factor between intrinsic gluinos and intrinsic charm, represented by G_C, may enhance the I$\widetilde{\rm G}$ contribution over that of IC because of the color octet nature of the gluino. However, in this work, to isolate mass effects, we assume the color factors for I$\widetilde{\rm G}$ are the same as IC, setting $G_C = 1$. Changing G_C would effectively scale the cross section ratio in Eq. (13) by a constant factor. The overall effect of changing G_C is small relative to the leading-twist cross section unless G_C is very large. The intrinsic charm mass is used as the scale from which to approximately evolve the intrinsic gluino cross section as previously done for intrinsic beauty [38]. Note that when $G_C = 1$, if $\widehat{m}_{\tilde{g}} = \widehat{m}_c$, the I$\widetilde{\rm G}$ and

IC cross sections are the same. The I$\widetilde{\text{G}}$ cross sections are normalized by scaling $P_{i\tilde{g}}$ in proportion to P_{ic}, as described below.

A limit of $P_{ic}^5 = 0.31\%$ was placed on the intrinsic charm probability in the five-particle state $|uudc\bar{c}\rangle$ by charm structure function data [50–52]. The higher Fock state probabilities were obtained from an estimate of double J/Ψ production [25,26], resulting in $P_{icc}^7 \sim 4.4\% P_{ic}^5$ [41]. Mass scaling was used to obtain the mixed intrinsic charm probabilities, $P_{iqc}^7 \sim (\widehat{m}_c/\widehat{m}_q)^2 P_{icc}^7$ [37]. To obtain the n-particle gluino Fock state probabilities, $P_{i\tilde{g}}^n$, we assume that the same relationships hold for the gluino states. The five-particle gluino state then scales as

$$P_{i\tilde{g}}^5 = \frac{\widehat{m}_c^2}{\widehat{m}_{\tilde{g}}^2} P_{ic}^5 \ . \tag{14}$$

Assuming $P_{i\tilde{g}\tilde{g}}^7 = 4.4\% P_{i\tilde{g}}^7$, the seven-particle Fock state probabilities are

$$P_{iq\tilde{g}}^7 = \frac{\widehat{m}_c^2}{\widehat{m}_q^2} P_{i\tilde{g}\tilde{g}}^7. \tag{15}$$

Thus, if $\widehat{m}_{\tilde{g}} = \widehat{m}_c$, $P_{ic}^5 = P_{i\tilde{g}}^5$ and $P_{icc}^7 = P_{i\tilde{g}\tilde{g}}^7$. For simplicity, the probability for the mixed gluon-gluino proton six-particle Fock state was set equal to the seven-particle mixed probability with $\widehat{m}_g = \widehat{m}_q$. The effective transverse masses used were $\widehat{m}_q = \widehat{m}_g = 0.45$ GeV, $\widehat{m}_s = 0.71$ GeV, and $\widehat{m}_c = 1.8$ GeV. The transverse mass of the gluino, $\widehat{m}_{\tilde{g}}$, is fixed to the values of $m_{\tilde{g}}$ used in the leading-twist calculation.

4. Composite model predictions

In this section, we calculate the total x_F distribution of final-state R-hadrons including both leading- and higher-twist contributions. The model predictions for R^+, R^0 and S^0 production on proton and nuclear targets are then given at 800 GeV.

The final-state $d\sigma/dx_F$ distribution is the sum of the leading-twist pQCD distribution and the higher-twist intrinsic contributions. Since many experiments use a nuclear target, the characteristic A dependence of each contribution is included,

$$\frac{d\sigma}{dx_F} = A\frac{d\sigma_{lt}}{dx_F} + A^\beta \frac{d\sigma_{i\tilde{g}}}{dx_F}. \tag{16}$$

The first term is the leading-twist term whereas the second term is the higher-twist I$\widetilde{\text{G}}$ contribution. Leading twist necessarily involves single parton interactions between the target and the projectile and thus cannot account for collective nuclear effects. Thus, the leading-twist cross section scales linearly with the number of nucleons in the target modulo nuclear shadowing effects. The nuclear dependence of J/ψ production in pA interactions shows that if the nuclear dependence is parameterized by A^α, $\alpha \to 2/3$ as $x_F \to 1$ [27–29]. The emergence of this surface effect at large x_F is consistent with spectators in the projectile coupling to soft gluons from the front face of the target rather than the volume. The NA3 collaboration extracted the A dependence of J/ψ production at large x_F and

obtained $\beta = 0.71$ in Eq. (16) [27]. We use the same value of β for charm production since the available data on the charm A dependence [53] leads us to expect a similar A dependence for charm and J/ψ production at large x_F.

The intrinsic gluino contribution to R-hadron production includes contributions from both hadronization of single gluinos by uncorrelated fragmentation, Eq. (7), and coalescence into final-state R-hadrons, described in Eqs. (8)–(10). That is,

$$\frac{dP^n_{i\tilde{g}}}{dx_F} = \xi_1 \frac{dP^{nF}_{i\tilde{g}}}{dx_F} + \xi_2 \frac{dP^{nC}_{i\tilde{g}}}{dx_F}, \tag{17}$$

where $P^{nF}_{i\tilde{g}}$ and $P^{nC}_{i\tilde{g}}$ are the $\widetilde{\mathrm{IG}}$ contributions from fragmentation and coalescence, respectively. The parameters ξ_1 and ξ_2 allow adjustment of the relative gluino fragmentation and coalescence contributions. We used single gluino fragmentation from the same Fock state as the coalesced hadron. That is, for R^+, $k = 5$ in Eq. (7), while $k = 6$ for R^0 and $k = 7$ for S^0. We fix $\xi_1 = \xi_2 = 0.5$ for simplicity. For a more realistic accounting of all possible contributions to Eq. (17) for charm production, see Ref. [42] for relative charm hadron production probabilities in the proton. The respective fragmentation and coalescence probability distributions in Eq. (17) are converted to cross sections using Eq. (11) and added to the leading-twist cross section as in Eq. (16).

We calculate R-hadron production at 800 GeV in pp, pBe, and pCu interactions with $m_{\tilde{g}} = \widehat{m}_{\tilde{g}} = 1.2$, 1.5, 3.5, and 5.0 GeV. Delta function fragmentation was used for single intrinsic gluino production by uncorrelated fragmentation and for leading-twist hadronization. That is, we take $D_{H/\tilde{g}}(z) = \delta(1-z)$ in Eqs. (1) and (7).

Fig. 3 shows the normalized R-hadron x_F distributions calculated according to Eq. (11) in pp interactions with $m_{\tilde{g}} = 1.2$ GeV. The difference in the yields as $x_F \to 0$ is due to the difference in probability for the five-, six-, and seven-particle Fock states. The R^0 and S^0 cross sections are similar at low x_F because we have assumed $P^6_{ig\tilde{g}} = P^7_{iq\tilde{g}}$, as described in the previous section. However, the shapes are different at low x_F because the probability distribution for uncorrelated fragmentation has a smaller average $\langle x_F \rangle$ when $k = 7$ in Eq. (7). The R^+ has the largest cross section of the three hadrons. Its distribution is symmetric around $x_F = 0.5$ because the fragmentation yield and the R^+ yield from coalescence are symmetric in the five-particle Fock state. The S^0 yield increases near $x_F \sim 0.25$ due to the forward peak of the S^0 coalescence distribution seen in Fig. 2. The yield at low x_F is relatively reduced because the fragmentation calculation with $k = 7$ is narrower so that the two peaks are effectively separated in Fig. 2. Since the fragmentation peak for $k = 6$ and the R^0 coalescence distribution lie close together, they blend into a broad peak for the R^0 x_F distribution.

Figs. 4, 5, and 6 show the predicted R^+, S^0, and R^0 x_F distributions per nucleon in pp, pBe, and pCu interactions at 800 GeV calculated according to Eq. (16). Each figure includes all four gluino masses. As $x_F \to 0$ the x_F distributions of all targets are equal for a given $m_{\tilde{g}}$. This indicates the dominance of leading-twist production at low x_F, independent of the final state. As $x_F \to 1$ the higher-twist terms begin to contribute. These higher-twist effects are suppressed in nuclear targets because of their slower relative growth as a function of A compared to the leading-twist A dependence. Although larger mass gluinos

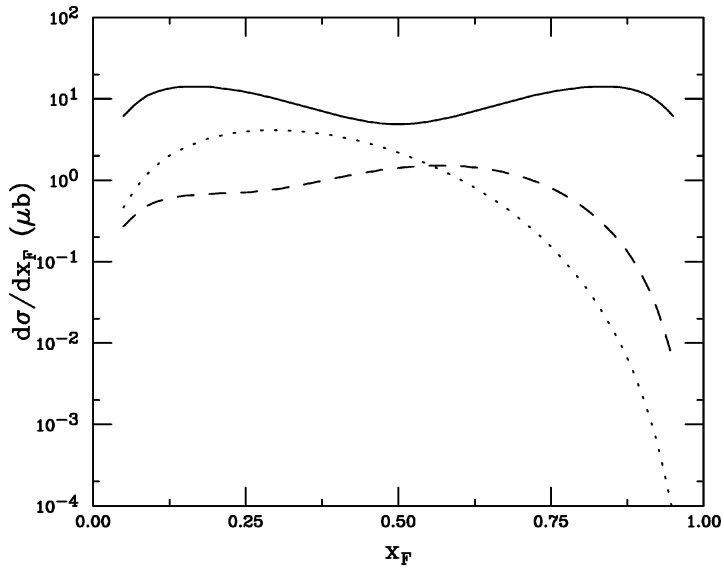

Fig. 3. Intrinsic gluino higher-twist contributions to $d\sigma_{i\tilde{g}}/x_F$ in R-hadron production with $m_{\tilde{g}} = 1.2$ GeV. The solid curve is R^+, the dotted curve is R^0, and the dashed curve is S^0. Each distribution includes the contribution from independent uncorrelated fragmentation of a gluino.

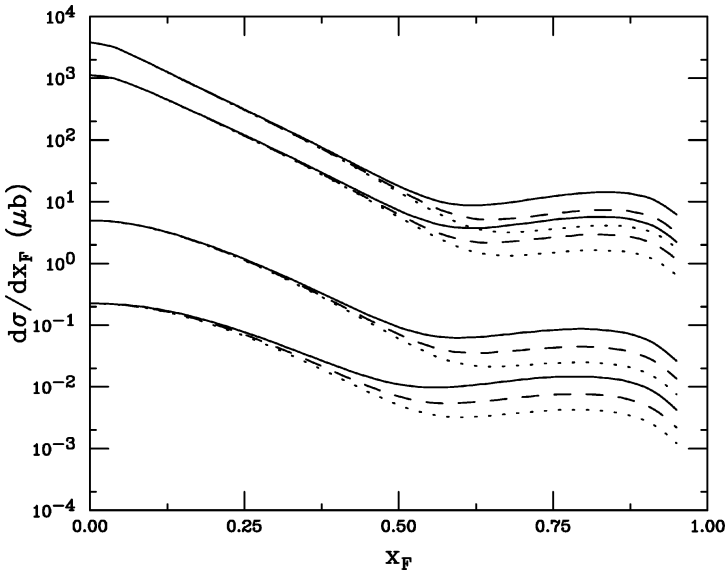

Fig. 4. R^+ x_F distribution from 800 GeV protons on various targets. Four gluino masses are chosen, $m_{\tilde{g}} = 1.2$ GeV (top), 1.5 GeV, 3.5 GeV, and 5.0 GeV (bottom). For each mass, there is a triplet of curves representing different targets: proton (solid), Be (dashed), and Cu (dotted).

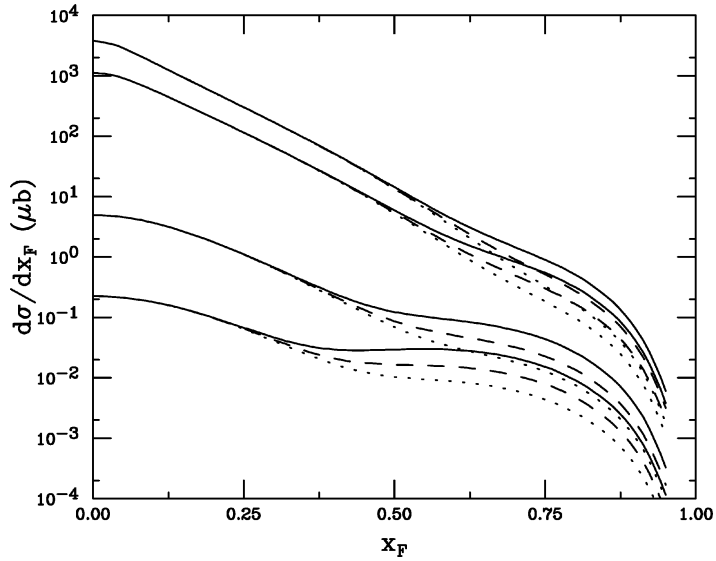

Fig. 5. S^0 x_F distribution from 800 GeV protons on various targets. Four gluino masses are chosen, $m_{\tilde{g}} = 1.2$ GeV (top), 1.5 GeV, 3.5 GeV, and 5.0 GeV (bottom). For each mass, there is a triplet of curves representing different targets: proton (solid), Be (dashed), and Cu (dotted).

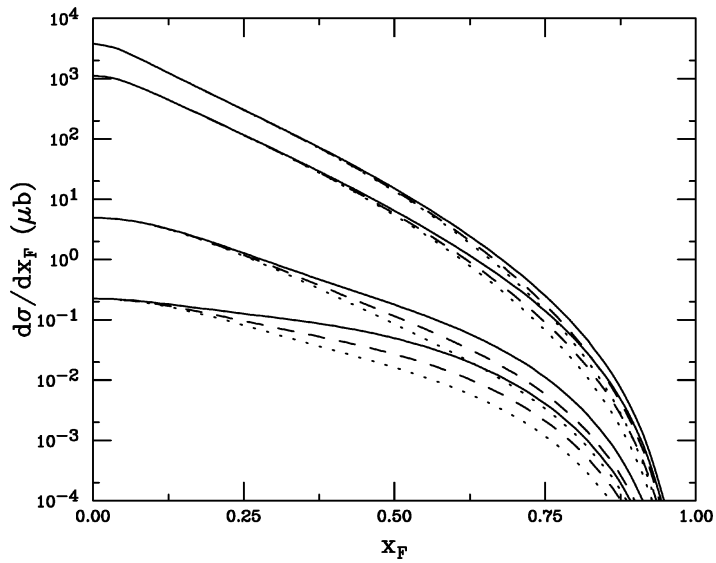

Fig. 6. R^0 x_F distribution from 800 GeV protons on various targets. Four gluino masses are chosen, $m_{\tilde{g}} = 1.2$ GeV (top), 1.5 GeV, 3.5 GeV, and 5.0 GeV (bottom). For each mass, there is a triplet of curves representing different targets: proton (solid), Be (dashed), and Cu (dotted).

are more difficult to create, the relative contribution to the total cross section from higher-twist production in Eq. (16) increases with gluino mass because of the slower decrease of the intrinsic gluino contribution relative to the mass suppression of the leading-twist cross section. The greater mass suppression of the leading-twist cross section also influences the value of x_F where the higher-twist contribution begins to appear. Increasing the gluino mass leads to intrinsic gluino effects appearing at lower x_F. This effect is seen in Figs. 4–6. When $m_{\tilde{g}} = 1.2$, I$\widetilde{\text{G}}$ effects become obvious near $x_F \sim 0.5$ while I$\widetilde{\text{G}}$ contributions begin to appear for $x_F \sim 0.12$ in R^0 production when $m_{\tilde{g}} = 5.0$ GeV.

Dramatic leading effects are predicted for the R^+ which, as pointed out above, shares three valence quarks with the proton in a minimal five-particle Fock state configuration. This characteristic "hardening" of the x_F distribution for $x_F > 0.6$ should be clear in a successful R^+ search. However, the leading effects are also present for the other particles. The S^0 is the next hardest distribution, sharing two valence quarks with the proton while the R^0 tends to be the softest, since no projectile valence quarks are shared.

For a clearer comparison of the leading effects predicted for each final-state R-hadron, Figs. 7–10 show the R^+, S^0, and R^0 distributions together in pp interactions with $m_{\tilde{g}} =$ 1.2, 1.5, 3.5, and 5.0 GeV, respectively. The leading-twist gluino distribution is also shown for comparison. In each case, the intrinsic contribution begins to emerge from the leading-twist calculation between $x_F \sim 0.12$ and $x_F \sim 0.4$. In Fig. 8, with $m_{\tilde{g}} = 1.5$ GeV, the predicted R^+ enhancement at $x_F \sim 0.8$ is about 700 times larger than the leading-twist prediction. At the same value of $m_{\tilde{g}}$ and x_F, the S^0 contribution is about 40 times greater while the R^0 is just under 6 times greater. When the gluino mass is increased to $m_{\tilde{g}} = 5.0$ GeV, shown in Fig. 10, the R^0 dominates R-hadron yields for $x_F < 0.6$. This is a consequence of the increased $\langle x_F \rangle$ for single gluino fragmentation at the larger mass. Although the cross sections are small at $m_{\tilde{g}} = 5.0$ GeV since the gluino mass is comparable to the bottom mass, the predicted enhancements over the leading-twist baseline are quite large: 1.9×10^4 for the R^+, 1.2×10^4 for the S^0, and 2.1×10^3 for the R^0. The enhancements are in fact larger than those with smaller gluino masses due to the greater mass suppression of the leading-twist cross section.

Finally, we compare and contrast our results with $m_{\tilde{g}} = 1.5$ GeV to those expected for intrinsic charm in pp interactions at 800 GeV. (Actual measurements of the charm distributions are not yet available, but we employ the same intrinsic formalism that successfully describes the leading charm distributions observed in $\pi^- A$ interactions [18–24].) It is useful to compare the charged D mesons: the $D^-(d\bar{c})$, which shares a valence quark with the proton and is therefore leading (L); and the $D^+(\bar{d}c)$, which must be produced by coalescence from a seven-particle Fock state and is nonleading (NL). The results are often expressed in terms of the asymmetry,

$$A(x_F) = \frac{d\sigma_L/dx_F - d\sigma_{NL}/dx_F}{d\sigma_L/dx_F + d\sigma_{NL}/dx_F}. \tag{18}$$

To compare our gluino calculations as directly as possible with the charm results, we consider both R^+ and R^- production. While R^+ production is leading, production of the $R^-(\bar{u}\,\bar{u}\,\bar{d}\,\tilde{g})$ barino (the R^+ anti-particle) will be nonleading in comparison. Indeed, to

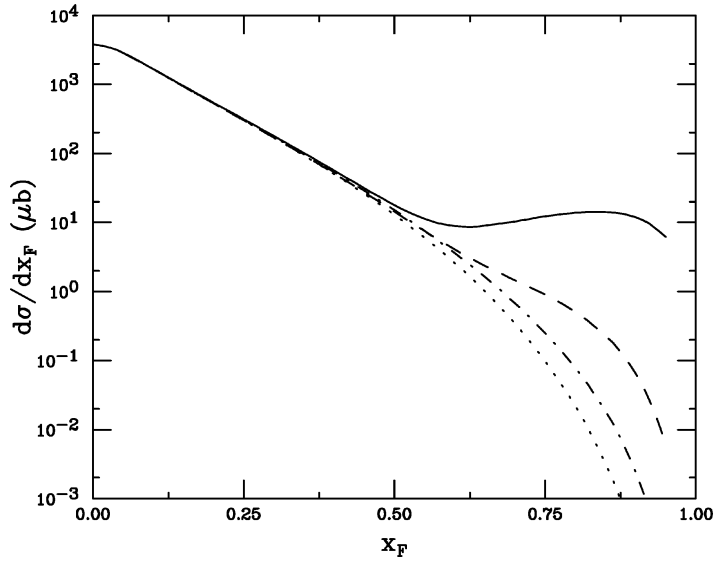

Fig. 7. Intrinsic gluino enhancement to x_F distribution for various R-hadrons with $m_{\tilde{g}} = 1.2$ GeV. The lower curve is the fusion baseline for gluino production with a delta function fragmentation. The curves are R^+ (solid), S^0 (dashed), R^0 (dot-dashed), and the leading-twist gluino production (dotted).

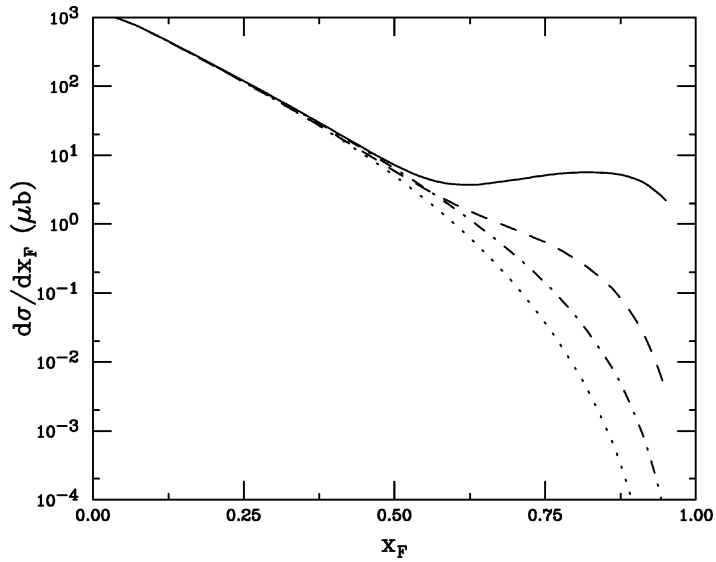

Fig. 8. Intrinsic gluino enhancement to x_F distribution for various R-hadrons with $m_{\tilde{g}} = 1.5$ GeV. The lower curve is the fusion baseline for gluino production with a delta function fragmentation. The curves are R^+ (solid), S^0 (dashed), R^0 (dot-dashed), and the leading-twist gluino production (dotted).

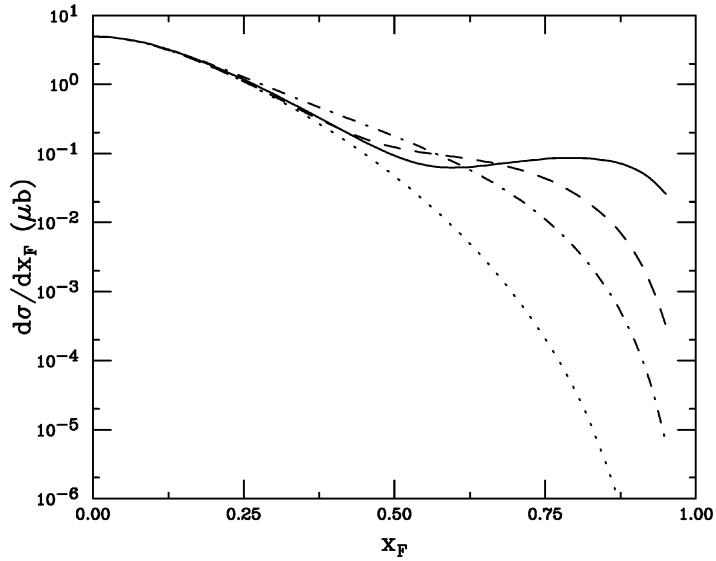

Fig. 9. Intrinsic gluino enhancement to x_F distribution for various R-hadrons with $m_{\tilde{g}} = 3.5$ GeV. The lower curve is the fusion baseline for gluino production with a delta function fragmentation. The curves are R^+ (solid), S^0 (dashed), R^0 (dot-dashed), and the leading-twist gluino production (dotted).

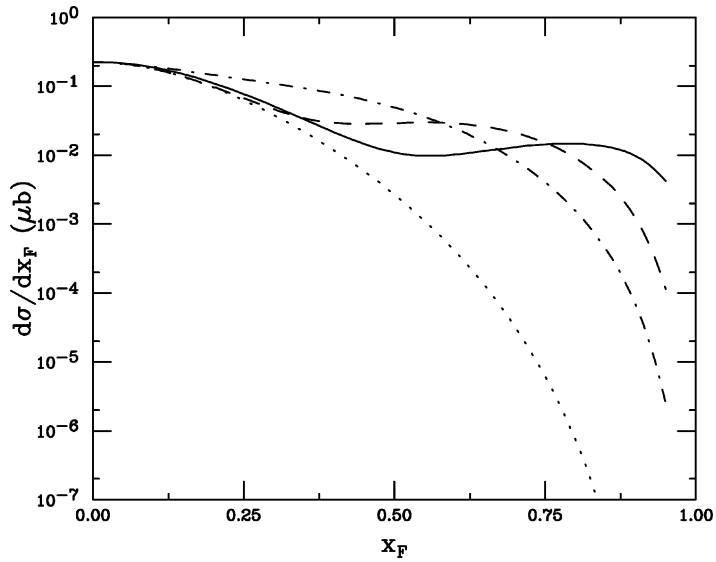

Fig. 10. Intrinsic gluino enhancement to x_F distribution for various R-hadrons with $m_{\tilde{g}} = 5.0$ GeV. The lower curve is the fusion baseline for gluino production with a delta function fragmentation. The curves are R^+ (solid), S^0 (dashed), R^0 (dot-dashed), and the leading-twist gluino production (dotted).

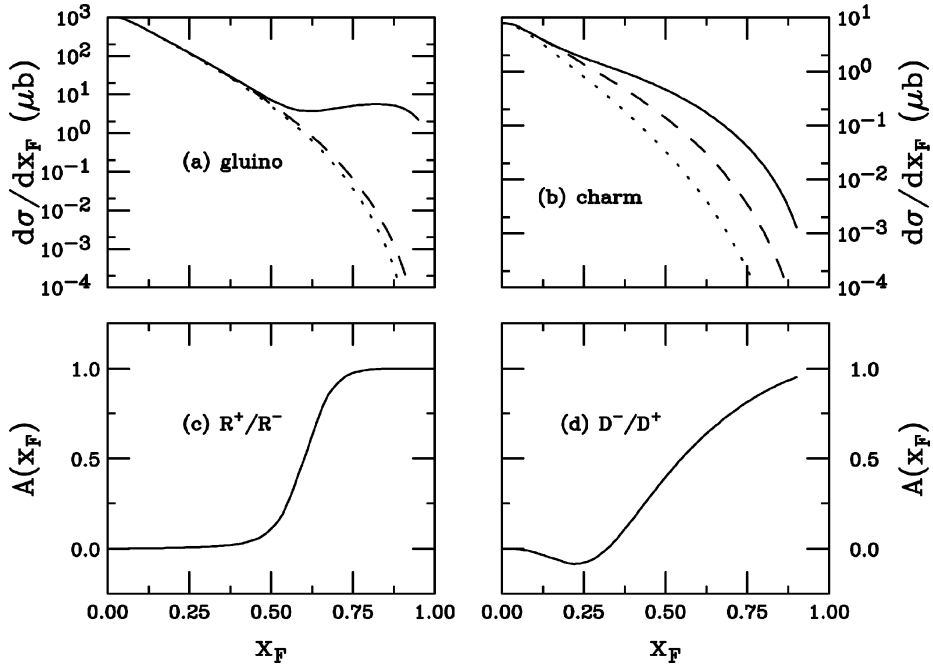

Fig. 11. We compare intrinsic gluino enhancements in pp interactions at 800 GeV to those predicted in charm production in the same reaction. In (a) we show the R^+ (solid), R^- (dashed), and fusion baseline (dotted) compared to (b) the D^- (solid), D^+ (dashed), and fusion baseline (dotted) as a function of x_F. The asymmetries between (c) R^+ and R^- and (d) D^- and D^+ are also shown.

first approximation, the only higher-twist intrinsic contribution to R^- production is that in which it comes from the fragmentation of an intrinsic gluino; coalescence production of the R^- requires an eleven-particle intrinsic state and is expected to be negligible.

The resulting distributions for the gluino and charm hadrons, as well as the corresponding asymmetries, are shown in Fig. 11. The R^- x_F distribution is only slightly enhanced over the leading-twist result. The charm distributions, calculated using the intrinsic charm model described in Ref. [42], show a greater separation between the D^- (solid), D^+ (dashed), and the leading-twist calculations. The D^- does not exhibit the strong leading behavior of the R^+ because it shares only one valence quark with the proton while the R^+ shares all three proton valence quarks. The charm model of Ref. [42] includes coalescence production from seven-particle Fock states of the proton, which could account for the substantial difference between the full- and leading-twist D^+ fusion curves in Fig. 11 as compared to the small difference between the full- and leading-twist R^- distributions (the eleven-particle intrinsic state coalescence contribution to R^- production being negligible, as noted earlier).

The asymmetry between the R^+ and R^- barinos is quite different than that between the D^- and D^+ mesons. The barino asymmetry is nearly zero until $x_F \sim 0.5$ and then rises sharply to unity. The charm meson asymmetry is predicted to be slightly negative at low x_F if the rates for the charged D meson production at leading twist are assumed to be equal,

then rising slowly toward unity as x_F increases. We note that we have chosen to compare the barino results to D mesons instead of charm baryons such as Λ_c and $\bar{\Lambda}_c$ since data on D production is more abundant. If we had chosen the Λ_c and $\bar{\Lambda}_c$, the results would have been similar to those for the R-hadrons.

5. Conclusions

The light gluino window opens the possibility of non-trivial higher-twist gluino contributions to the proton wave function. In analogy to charm hadroproduction, intrinsic gluino Fock components contribute to final-state R-hadron formation, enhancing gluino production over leading-twist parton fusion in the forward x_F region.

In this work, we have studied a "maximally leading" scenario for final-state R-hadrons in pp and pA interactions at 800 GeV. Our model predicts that the contributions of higher-twist intrinsic states lead to strong flavor correlations between initial and final states for $x_F > 0.6$. The large intrinsic gluino enhancements at high x_F over the leading-twist predictions imply that this region of phase space could be especially appropriate for R-hadron searches in the light gluino scenario. For $m_{\tilde{g}}$ in the $1-5$ GeV range, a mass region where substantial evidence for the analogous intrinsic heavy quark states exists and for which our computational techniques should be most reliable, the enhancements are very significant (factors of several hundred to several thousand being common). The magnitudes we predict for these enhancements may even be conservative since the increased color factor associated with intrinsic gluinos compared to intrinsic charm has been neglected. These enhancements will, in turn, lead to large enhancements in the high x_F ρ, π, and Λ abundancies since they are decay products of the R-hadrons.

Acknowledgements

We would like to thank S.J. Brodsky for discussions.

References

[1] G.R. Farrar, Phys. Rev. Lett. 51 (1995) 3904.
[2] G.R. Farrar, Phys. Rev. Lett. 76 (1996) 4111.
[3] C.H. Chen, M. Drees, J.F. Gunion, Phys. Rev. D 55 (1997) 330.
[4] S. Raby, Phys. Rev. D 56 (1997) 2852.
[5] S. Raby, Phys. Lett. B 42 (1998) 158.
[6] G.R. Farrar, Nucl. Phys. Proc. Suppl. 62 (1998) 485.
[7] A. Alavi-Harati et al., KTeV Collaboration, Phys. Rev. Lett. 83 (1999) 2128.
[8] J. Adams et al., KTeV Collaboration, Phys. Rev. Lett. 79 (1997) 4083.
[9] I.F. Albuquerque et al., E761 Collaboration, Phys. Rev. Lett. 78 (1997) 3252.
[10] P.M. Tuts et al., Phys. Lett. B 186 (1987) 233.
[11] F. Csikor, Z. Fodor, Phys. Rev. Lett. 78 (1997) 4335.

[12] F. Csikor, Z. Fodor, in: D. Lellouch, G. Mikenberg, E. Rabinovici (Eds.), Proc. High Energy Physics, Jerusalem, 1997, pp. 883–886, hep-ph/9712269.
[13] Z. Nagy, Z. Trocsanyi, hep-ph/9708343.
[14] P. Abreu et al., DELPHI Collaboration, Phys. Lett. B 414 (1997) 410.
[15] R. Barate et al., ALEPH Collaboration, Z. Phys. C 96 (1997) 1.
[16] L. Clavelli, UA-HEP-99-4; hep-ph/9908342.
[17] H. Baer, K. Cheung, J.F. Gunion, Phys. Rev. D 59 (1999) 075002.
[18] E.M. Aitala et al., E791 Collaboration, Phys. Lett. B 371 (1996) 157.
[19] M. Aguilar-Benitez et al., LEBC-EHS Collaboration, Phys. Lett. 161B (1985) 400.
[20] M. Aguilar-Benitez et al., LEBC-EHS Collaboration, Z. Phys. C 31 (1986) 491.
[21] S. Barlag et al., ACCMOR Collaboration, Z. Phys. C 49 (1991) 555.
[22] M.I. Adamovich et al., WA82 Collaboration, Phys. Lett. B 305 (1993) 402.
[23] G.A. Alves et al., E769 Collaboration, Phys. Rev. Lett. 72 (1994) 812.
[24] M.I. Adamovich et al., WA89 Collaboration, Eur. Phys. J. C 8 (1999) 93.
[25] J. Badier et al., NA3 Collaboration, Phys. Lett. 114B (1982) 457.
[26] J. Badier et al., NA3 Collaboration, Phys. Lett. 158B (1985) 85.
[27] J. Badier et al., NA3 Collaboration, Z. Phys. C 20 (1983) 101.
[28] D.M. Alde et al., E772 Collaboration, Phys. Rev. Lett. 66 (1991) 133.
[29] M.J. Leitch et al., E866 Collaboration, Phys. Rev. Lett. 84 (2000) 3256.
[30] J.C. Collins, D.E. Soper, G. Sterman, in: A.H. Mueller (Ed.), Perturbative QCD, World Scientific, Singapore, 1989.
[31] G. Bodwin, Phys. Rev. D 31 (1985) 2616.
[32] G. Bodwin, Phys. Rev. D 34 (1986) 3932.
[33] J. Qiu, G. Sterman, Nucl. Phys. B 353 (1991) 105.
[34] S.J. Brodsky, C. Peterson, N. Sakai, Phys. Lett. B 93 (1980) 451.
[35] S.J. Brodsky, C. Peterson, N. Sakai, Phys. Rev. D 23 (1981) 2745.
[36] S.J. Brodsky, J.F. Gunion, D.E. Soper, Phys. Rev. D 36 (1987) 2710.
[37] R. Vogt, S.J. Brodsky, Nucl. Phys. B 478 (1996) 311.
[38] R. Vogt, S.J. Brodsky, Nucl. Phys. B 438 (1994) 261.
[39] R. Vogt, S.J. Brodsky, P. Hoyer, Nucl. Phys. B 360 (1991) 67.
[40] R. Vogt, S.J. Brodsky, P. Hoyer, Nucl. Phys. B 383 (1992) 643.
[41] R. Vogt, S.J. Brodsky, Phys. Lett. B 349 (1995) 569.
[42] T. Gutierrez, R. Vogt, Nucl. Phys. B 539 (1999) 189.
[43] S. Dawson, E. Eichten, C. Quigg, Phys. Rev. D 31 (1985) 1581.
[44] A.D. Martin, W.J. Stirling, R.G. Roberts, Phys. Lett. B 306 (1993) 145.
[45] S.J. Brodsky, P. Hoyer, A.H. Mueller, W.-K. Tang, Nucl. Phys. B 369 (1992) 519.
[46] W.-K. Tang, in: D.M. Kaplan, S. Kwan (Eds.), The Future of High Sensitivity Charm Experiments, Batavia, IL, 1994, pp. 251–266, hep-ph/9408372.
[47] P. Hoyer, Acta Phys. Pol. B 23 (1992) 1145.
[48] G.P. Lepage, S.J. Brodsky, Phys. Rev. D 22 (1980) 2157.
[49] The factor of $1/z$ associated with the fragmentation function was left out in Refs. [37,38,40,42]. However, the factor was included in computing the numerical results given in these papers.
[50] J.J. Aubert et al., EMC Collaboration, Phys. Lett. 110B (1982) 73.
[51] E. Hoffmann, R. Moore, Z. Phys. C 20 (1983) 71.
[52] B.W. Harris, J. Smith, R. Vogt, Nucl. Phys. B 461 (1996) 181.
[53] J.A. Appel, Ann. Rev. Nucl. Part. Sci. 42 (1992) 367.